

## 7. SITE 924<sup>1</sup>

### Shipboard Scientific Party<sup>2</sup>

#### HOLE 924B

**Date occupied:** 14 January 1994  
**Date departed:** 16 January 1994  
**Time on hole:** 2 days, 09 hr, 05 min  
**Position:** 23°32.466'N, 45°0.864'W  
**Bottom felt (drill-pipe measurement from rig floor, m):** 3176.0  
**Distance between rig floor and sea level (m):** 11.30  
**Water depth (drill-pipe measurement from sea level, m):** 3164.7  
**Total depth (from rig floor, m):** 3206.80  
**Penetration (m):** 30.80  
**Number of cores (including cores having no recovery):** 5  
**Total length of cored section (m):** 40.80  
**Total core recovered (m):** 3.27  
**Core recovery (%):** 13.8  
**Hard rock:**  
Depth (mbsf): 30.80  
Nature: Olivine gabbro, gabbro, troctolite  
Measured velocity (km/s): 5.34–5.52

#### HOLE 924C

**Date occupied:** 16 January 1994  
**Date departed:** 20 January 1994  
**Time on hole:** 3 days, 13 hr, 30 min  
**Position:** 23°32.496'N, 45°0.864'W  
**Bottom felt (drill-pipe measurement from rig floor, m):** 3177.0  
**Distance between rig floor and sea level (m):** 11.30  
**Water depth (drill-pipe measurement from sea level, m):** 3165.7  
**Total depth (from rig floor, m):** 3225.50  
**Penetration (m):** 48.50  
**Number of cores (including cores having no recovery):** 7  
**Total length of cored section (m):** 33.8  
**Total core recovered (m):** 8.22  
**Core recovery (%):** 24.3  
**Hard rock:**  
Depth (mbsf): 48.50  
Nature: Olivine gabbro, gabbro, troctolite  
Measured velocity (km/s): 5.29–5.76

**Principal results:** Site 924 is located on the western median valley wall of the Mid-Atlantic Ridge at 23°32.47'N, 45°0.88'W, about 6 km south of the Kane Fracture Zone, and 1.7 km east and downslope from Sites 921 and 923

(Fig. 4, "Introduction," this volume). All three holes at this site were spudded into or near outcrops with a slabby to schistose appearance characteristic of plutonic rocks in the MARK area (Karson and Dick, 1983; Mével et al., 1991). There was no recovery from Hole 924A, but Hole 924B penetrated to a depth of 30.8 m and recovered 3.27 m of core for a cumulative recovery of 13.8%. Hole 924C, located about 20 m to the north, reached a depth of 33.8 m, recovered 8.22 m with a cumulative recovery of 24.3%.

In each hole, a single rock unit was designated, consisting of varying proportions of weakly deformed and variably altered olivine gabbro to troctolite. The rocks are compositionally and texturally heterogeneous on the scale of centimeters to meters with well developed compositional and grain-size layering.

Rocks from Hole 924B are generally olivine gabbro. In detail they are interlayered gabbro and poikilitic olivine gabbro. These rocks have a greater proportion of brown to green clinopyroxene than similar rock units recovered from nearby sites drilled during Leg 153. In addition, some of the brown clinopyroxene occurs as a cumulate phase.

Olivine gabbro recovered from Hole 924B is characterized by cumulus olivine with local crescumulus textures and by large (up to 6 cm) poikilitic grains of green clinopyroxene. Moderately dipping, diffuse modal layering is common. Gabbro from this hole is notable for its green poikilitic clinopyroxene and brown cumulus clinopyroxene. The coexistence of these two textural types of clinopyroxene was not observed in other gabbroic rocks recovered from Sites 921–923. The Site 924 rocks may be transitional in character between two of the common rock types recovered elsewhere in this area: gabbro with brown clinopyroxene and poikilitic olivine gabbro.

Hole 924C intersected a sequence of poikilitic olivine gabbro and troctolite bearing green poikilitic clinopyroxene. Fine-scale, modal layering is common in this rock type, and locally coincides with grain-size layering, a relationship that is only rarely observed in poikilitic olivine gabbro cored at Sites 921–923. Locally, this layering is very similar in appearance to that in the interval defined as Unit 3 from the core recovered from Hole 923A. Layering within the core from Hole 924B is typically moderately to steeply dipping and varies from centimeters to decimeters in scale. Olivine occurs as a ubiquitous cumulus phase in these rocks and locally has a crescumulus morphology.

Alteration of the gabbroic rocks from Holes 924B and 924C is closely related to the compositional variations and specifically to the modal content of olivine. Overall the olivine gabbro recovered from both holes is variegated green to gray and moderately to intensely altered, typically 15%–30%, but locally reaching 90%. Troctolitic intervals, which are present mainly in the core from Hole 924C, have a mottled green color and a consistently higher degree of alteration, commonly near 90%. The specific alteration of different mineral phases is similar in both rock types. Olivine is typically partially replaced by talc and iron oxide minerals. Along contacts with plagioclase grains, coronas of various minerals are developed. In some cases, these reach 1–2 mm in width and are composite structures with parallel bands of one or more of the following minerals: tremolite, talc, chlorite. Dark chlorite coronas generally form the outer bands and tend to highlight the shapes of olivine grains, emphasizing igneous and deformational fabrics. Clinopyroxene, where present, is partially replaced by actinolite and trace amounts of brown hornblende. Plagioclase grains are overgrown by chlorite in olivine gabbro and intensely altered to clay minerals in troctolite. This general alteration style is very similar to that observed in gabbroic and troctolitic rocks recovered from Hole 922A.

<sup>1</sup> Cannat, M., Karson, J.A., Miller, D.J., et al., 1995. *Proc. ODP, Init. Repts.*, 153: College Station, TX (Ocean Drilling Program).

<sup>2</sup> Shipboard Scientific Party is given in the list of participants preceding the contents.

The rocks recovered at Site 924 show only weak manifestations of deformation. Inequant plagioclase and olivine grains define weak foliations and lineations. Crystal-plastic deformation has affected the rock only locally and is generally weak. In hand specimen it was difficult to distinguish between magmatic shape preferred orientations and this weak tectonic fabric. Crystal-plastic foliations and lineations are generally steeply dipping and plunging and locally flatten into subhorizontal orientations. Foliated and/or lineated domains, 20–30 cm wide, have gradational boundaries and no sharply bounded shear zones are present. The distribution of deformation through the cores is non-systematic, but there is a slight increase in the development of deformation fabrics toward the lowermost part of the core from Hole 924C.

Brittle deformation structures are also sparse in the rocks from both holes at Site 924. Localized zones of distributed cracks form dense networks, some of these have closely spaced parallel hairline fractures or veins. Cataclastic fault zones up to 3 cm wide both predate and postdate greenschist facies metamorphism. The pre-metamorphic fault zones are overgrown by a dense mesh of acicular tremolite-actinolite. Despite the intense alteration of the core, veining is sparse. Still, at least three generations of veins have been tentatively identified on the basis of crosscutting relationships and mineralogies. They include veins of actinolite, actinolite + chlorite, and clay minerals + epidote. Prehnite and epidote also occur locally.

Paleomagnetic studies on half-cores and discrete minicore samples of gabbroic rocks from Holes 924B and 924C reveal high-stability components of dominantly shallow (0° to 30°), positive inclinations after demagnetization to 20 mT. However, shallow negative components (to -30°) are present in some intervals of the core. The multiple components suggest the possibility of intimately mixed intervals of different polarities. No systematic pattern of magnetization is obvious from the presently available data.

The physical properties of rocks recovered from Site 924 are almost identical to those obtained from Site 922. Density, velocity, and porosity are somewhat less than were observed in rocks recovered from Sites 921 and 923, and thermal conductivities in rocks recovered from Sites 922 and 924 are considerably greater than those observed in rock recovered from Sites 921 and 923. These results are all in accord with the comparatively higher extents of alteration at Sites 922 and 924 than at Sites 921 and 923.

## OPERATIONS

### Site 923 Transit to Site 924

The vessel was offset approximately 1.5 km to the east as the drill string was being recovered from Hole 923A. A positioning beacon was deployed at 0408 hr, 13 January, initiating Site 924.

### Hole 924A

After recovering the drill string from Hole 923A, a new bottom hole assembly (BHA) was assembled. The BHA was tripped to the seafloor followed by the VIT and a seafloor survey was begun. A spud site was located and the bit set on the seafloor. The bit was jetted in 0.5 m with 375 gpm and 8000 lb weight on bit (WOB). The seafloor depth was determined by drill-pipe measurement to be 3170 mbrf (3158.7 mbsl). The VIT was retrieved and Hole 924A was spudded at 1724 hr, 13 January.

The hole was cored to 3180 mbrf (10 mbsf) when the drill collar immediately above the outer core barrel failed through the zip lift groove. The failure occurred 12 m above the seafloor at 0230 hr, 14 January, ending Hole 924A.

### Hole 924B

A new BHA was run in the hole, followed by the VIT. A 2 hr seafloor survey was conducted. The vessel was offset 15 m west of Hole 924A and the bit set on bottom. The bit was jetted 0.5 m at 375 gpm and 8000 lb WOB. As the VIT was being retrieved in preparation for spudding Hole 924B, the bit skidded downhill.

The bit was picked up clear of the seafloor as the VIT was run back to bottom. The vessel was offset 15 m east of Hole 924A where the bit was set on bottom once again. A similar jet test was performed with similar results. The VIT was retrieved and Hole 924B was spudded at 2133 hr, 14 January. The seafloor depth was determined by drill-pipe measurement to be 3176 mbrf (3164.7 mbsl).

Hole 924B was cored three times to a depth of 3206.8 mbrf (30.8 mbsf) recovering 2.69 m of gabbro (Table 1). High torque and long reaming times in conjunction with recovering small amounts of highly fractured material resulted in the decision to abandon the hole.

The bit was pulled clear of the seafloor at 1135 hr, 16 January, ending Hole 924B.

### Hole 924C

With the drill string already down, the VIT was deployed and a 2 hr seafloor survey was conducted. The first spud attempt resulted in the bit skidding downhill. Another spud site was chosen next to a cliff. The bit was set on bottom and a jet test performed. During the jet test the bit cones could be seen as water was pumped between them. The vessel heaved and the bit skidded into a small crack. The VIT was retrieved and Hole 924C was spudded at 1500 hr, 16 January.

The seafloor depth at Hole 924C was determined by drill-pipe measurement to be 3177 mbrf (3165.7 mbsl). Hole 924C was cored seven times to a depth of 3225.5 mbrf (48.5 mbsf), recovering 8.22 m of gabbro. Few hole problems were encountered.

With expiration of allotted coring time for the leg, the hole had to be abandoned. Hole 924C ended at 0500 hr, 20 January, when the bit cleared the rotary table.

### Camera Survey

The VIT camera and sonar survey for Site 924 was conducted on the slopes of the western rift valley wall of the MAR east of Sites 921 and 923 (see Fig. 4, "Introduction," this volume). It lasted 4 hr and explored an area where gabbroic outcrops had previously been identified during a *Nautila* dive (Auzende et al., 1993). The survey began at a positioning beacon that was dropped at 23°32.00'N and 45°01'W (Fig. 1). From this point, at a depth of 3320 mbsl (estimated from the length of the drill pipe), the traverse proceeded up hill to the west over a gently dipping muddy to rubbly slope, littered with decimeter- to meter-size blocks inferred to be gabbro (based on submersible sampling in the area). The survey continued to the west and upslope until it reached an area of steeper topography at about 3220 mbsl, with either very large (10–20 m) blocks or discontinuous outcrops of massive, gabbroic(?) rocks protruding from a relatively thick mud blanket. Moving parallel to contours to the north, more unambiguous outcrops were encountered. These are characterized by a slabby to schistose appearance that is characteristic of plutonic rocks in the MARK area. Estimates of local slopes were not made during this survey because the positioning beacon on the VIT frame was not working. Test tagging in a sediment pond on a steep outcrop face produced a cloud of mud that flowed rapidly downslope, which suggested that the slope was too steep for unsupported spudding. Upslope to the west, the outcrops appear to be buried beneath a continuous mantle of mud and rubble. This muddy area was explored upslope to about 3120 mbsl, at which point the decision was made to find a sufficiently gently sloping surface for unsupported drilling in the previously explored outcrops. Further test tagging revealed an area with a slope that was considered drillable and Hole 924A was spudded in less than 1 m of mud, on the outcrop face at a depth of 3170 mbsl.

After the BHA sheared off in Hole 924A, a second drilling target was chosen 12 m away following a very brief reconnaissance of the drilling area with the VIT camera. Hole 924B was abandoned as a result of rapidly degrading hole conditions and another brief VIT and sonar survey was conducted to locate a new target. This survey began

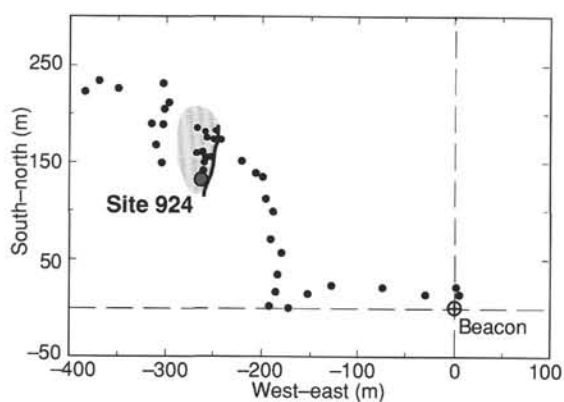


Figure 1. Map of the area surveyed with the VIT camera and sonar for locating Site 924 (Holes 924A–C: 23°32.47'N, 45°0.88'W). Bold dots indicate locations where depths were estimated from the total length of the drill string. Shaded areas = outcrops; thick line = inferred fault.

with a short traverse to the south that encountered only smooth muddy seafloor. Returning to Holes 924A and 924B and continuing about 20 m to the north, a series of steep, rugged cliff faces were encountered. After a brief examination of these outcrops, Hole 924C was spudded at a depth of 3177 mbsf. The drill bit was placed on a small bench on the shoulder of a very steep, rugged outcrop surface. The drill bit slid into a small crevice and the hole was spudded. The surrounding outcrops are typical of those described from submersible studies in the area (Karson and Dick, 1983; Mével et al., 1991; Auzende et al., 1993). These have extensive east-dipping platy, striated surfaces interpreted as dip-slopes on major faults or shear zones that are truncated by a steep cliff face. The hole was spudded near the base of a cliff and therefore structurally below the best developed fault surfaces.

### Lithologic Units

At the three holes drilled at Site 924, a total of 14.46 m of gabbroic rock were recovered from a total depth of penetration of 79.3 mbsf. No core was recovered from Hole 924A and only 3.27 m of core came from Hole 924B. The remaining 11.19 m of core was recovered from Hole 924C, which was drilled about 20 m to the north of the previous two holes. The rocks recovered in these relatively short cores were sufficiently uniform to be designated as single units (Table 2; Fig. 2).

Like rocks recovered from nearby Sites 921, 922, and 923, variably deformed and altered gabbroic rocks recovered at Site 924 reflect the interplay of igneous, metamorphic, and tectonic processes on the slow-spreading Mid-Atlantic Ridge. Igneous processes have produced a wide range of magmatic textures and compositions that reflect incremental accretion of crustal material by the intrusion and crystallization of plutonic rock masses. If they have not been tectonically rotated, the moderately to steeply dipping modal and grain-size layering, cumulate textures, and magmatic flow fabrics suggest crystallization along steeply inclined walls of magma bodies of unknown dimensions. Crystal-plastic deformation that affected the rocks at near magmatic temperatures produced variable, but weak deformation fabrics in the rocks recovered from Site 924. Typically, in similar oceanic rocks, alteration and brittle deformation are coincident. In the rocks from Site 924, like those from Site 922 2 km away, intense alteration has occurred without extensive fracturing.

Together with the rocks from the nearby sites drilled into the gabbro terrane of the western median valley wall of the MAR, the rocks from Site 924 begin to delineate the scale upon which major variations in seafloor spreading processes operate. The rocks recovered from Holes 924B and 924C come from nearly 2 km closer to the MAR axis than those from the other Leg 153 sites, and therefore, assuming the simplest, symmetrical spreading history, might be as

Table 1. Coring summary, Holes 924B and 924C.

Core	Date (Jan. 1994)	Time (UTC)	Depth (mbsf)	Cored (m)	Recovered (m)	Recovery (%)
153-924B-						
1W	15	0730	0.0–11.3	11.3	0.00	
2R	15	1045	11.3–15.8	4.5	0.43	9.6
3R	15	1605	15.8–21.3	5.5	0.92	16.7
4W	16	0410	11.3–21.3	10.0	0.58	
5R	16	1400	21.3–30.8	9.5	1.34	14.1
Coring totals				19.5	2.69	13.8
Washing totals				21.3	0.58	
Combined totals				40.8	3.27	
153-924C-						
1R	17	0745	0.0–9.9	9.9	1.03	10.4
2R	18	0115	9.9–19.6	9.7	2.54	26.2
3R	18	0745	19.6–24.4	4.8	2.08	43.3
4R	18	2100	24.4–29.1	4.7	0.88	18.7
5R	19	0450	29.1–33.8	4.7	1.69	35.9
Coring totals				33.8	8.22	24.3

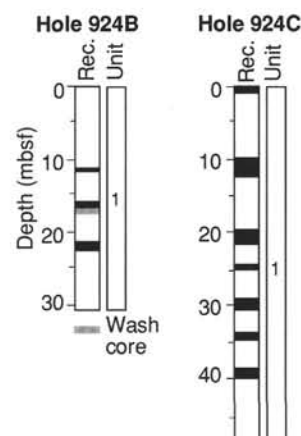


Figure 2. Columnar section showing the downhole recovery and lithological units in Holes 924B and 924C. Black indicates intervals recovered.

much as 100,000 yr younger. Thus, it is possible that variations in the character of the rocks recovered from these sites may reflect temporal variations in spreading processes.

Hole 924B intersected an interlayered sequence of lineated gabbro to olivine gabbro and olivine gabbro to troctolite that was designated as a single unit (Table 2). Recovery was poor and it is difficult to determine the relationship, if any, to rocks recovered at Sites 921, 922, and 923. The lineated gabbro is typical of the similar units recovered from holes at Site 921 and is characterized by the presence of brown cumulus clinopyroxene and a moderately developed mineral lineation defined the elongate habit of deformed clinopyroxene grains. The layering dips moderately to steeply.

Olivine gabbro is characterized by the presence of cumulus olivine, locally with a crescumulus habit, and by the presence of large (up to 6 cm) poikilitic grains of green clinopyroxene. Moderately dipping, diffuse, modal layering is common in this rock type. Undeformed gabbro in this hole is notable for containing both green poikilitic clinopyroxene and brown cumulus clinopyroxene. The existence of both of these textural types of clinopyroxene in the same rock has not been observed elsewhere within the gabbroic rocks recovered at sites drilled during Leg 153, and suggests that some of the gabbroic rocks at this site are transitional in character between brown clinopyroxene-bearing gabbro and the poikilitic olivine gabbro.

Hole 924C intersected a sequence of poikilitic olivine gabbro and troctolite that is characterized by the presence of green poikilitic clinopyroxene (Fig. 3). Only one unit was defined for rocks recovered from this hole (Table 2). Fine-scale, modal layering is common in this rock type (Fig. 4), but the local occurrence of both modal and grain-size

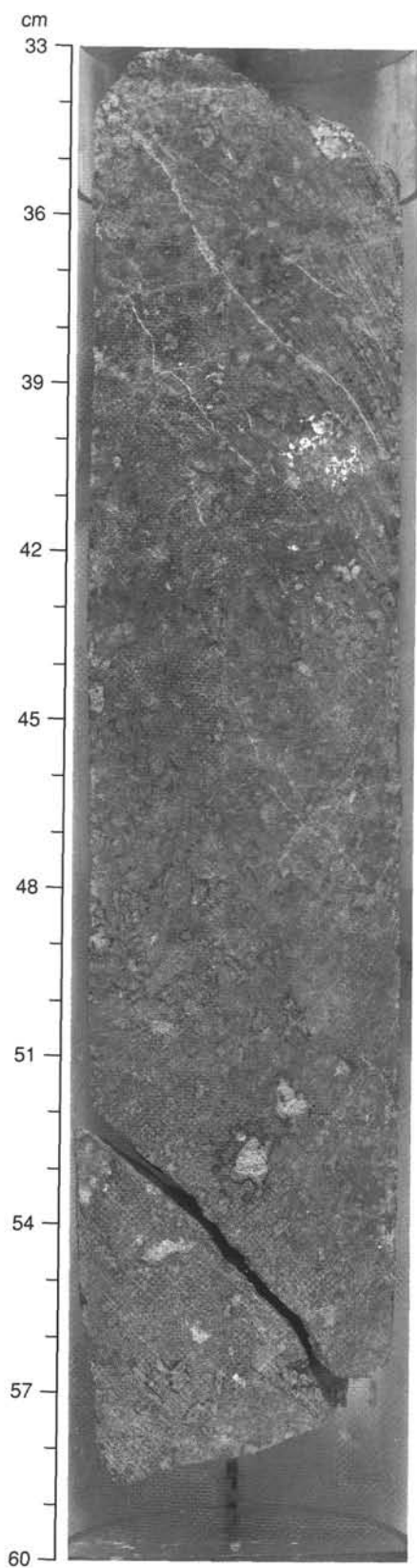


Figure 3. Poikilitic olivine gabbro to troctolite with green clinopyroxene. This rock type is typical of the single rock unit defined for rocks recovered from Hole 924C. Sample 153-924C-3R-2, 33–60 cm.

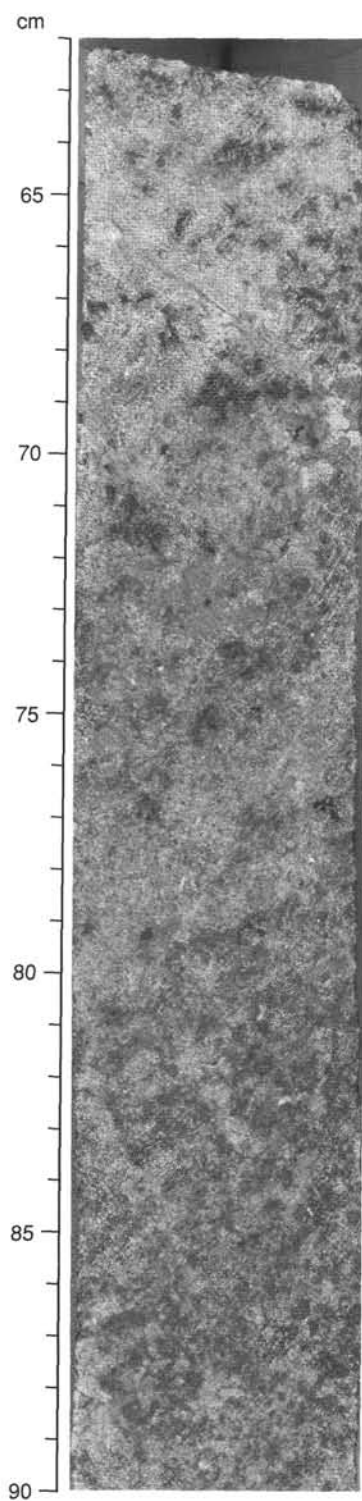


Figure 4. Typical fine-scale modal layering in poikilitic olivine gabbro from Hole 924C. Sample 153-924C-3R-1, 62–90 cm.

layering is rare for poikilitic olivine gabbro intersected in holes drilled at other sites during Leg 153. The best development of layering of this style is in a very coarse-grained layer that is similar in appearance to that defined as Unit 3 in Hole 923A. Layering within rocks from Hole 924C is typically moderately to steeply dipping, and varies in scale from centimeters to tens of centimeters in scale. Olivine is always a cumulus phase in these rocks, and it is locally crescumulus.

**Table 2. Summary of lithologic units defined for Holes 924B and 924C.**

Hole	Unit	Name	Cored interval		Curatorial depth to top of unit (mbsf)	Recovered (m)	Recovery (approx. %)
			From	To			
924B	1	Lineated gabbro/olivine gabbro	1R-1(1)	5R-1(13)	0.0	2.69	8.7
924C	1	Poikilitic olivine gabbro/troctolite	1R-1(1)	7R-1(6)	0.0	11.19	23.1

Notes: Percent recovery excludes wash core 153-924A-4W. Total depths of penetration were 30.8 mbsf for Hole 924B and 48.5 mbsf for Hole 924C.

## IGNEOUS PETROLOGY

### Lithologic Description

Site 924 drilling recovered a highly altered and texturally variable sequence of olivine-bearing gabbroic rocks. Alteration has resulted in the partial to pervasive replacement of the primary igneous mineralogy, particularly within the olivine-rich rocks. The following discussion describes the primary igneous characteristics. The observations presented in this report come from the macroscopic core description; no thin sections or XRF samples were taken from core recovered from this site because this coring occurred late in the cruise.

The range of rock types recovered at Holes 924B and 924C is more restricted than at Sites 921, 922, and 923. In particular, troctolite and olivine gabbro are the most commonly recovered lithologies. Gabbro was recovered in only one short (20 cm), highly deformed interval in Hole 924B. More evolved rock types (i.e., gabbro-norite, oxide gabbro, and diorite to trondhjemite) were not recovered. Two principal rock types were identified in Holes 924B and 924C: lineated gabbro and poikilitic olivine gabbro (Table 2). These are mineralogically similar to the predominant lithologies from previous sites (see "Igneous Petrology" sections, Sites 921–923, this volume) and will be discussed briefly.

#### Lineated Gabbro

The lineated gabbro recovered at Site 924 includes intimately mixed gabbro and olivine gabbro and is similar to lineated gabbro described from Site 921 and Site 923 in that the dominant characteristics are the presence of brown clinopyroxene and plagioclase as cumulus phases and the presence of a shape-preferred orientation defined by elongate clinopyroxene grains. This fabric is tectonic in origin. The descriptions of this rock type given in the Site 921 and Site 923 reports apply to rocks recovered from Site 924.

Lineated gabbro is predominantly medium- to coarse-grained and consists of 20% to 40% brown clinopyroxene, 3% to 20% olivine, and 55% to 70% plagioclase. Plagioclase is typically moderately recrystallized and rarely preserves a primary igneous texture. Clinopyroxene ranges from anhedral to relict euhedral in shape, and it is porphyroclastic in relatively strongly deformed samples. The crystal-plastic fabric is moderately to steeply dipping. While most pieces of core recovered from Hole 924B are small, igneous grain-size layering on the scale of 2 to 5 cm is present in larger pieces.

#### Poikilitic Olivine Gabbro

The extent of alteration in olivine gabbro is substantial, such that description of the primary igneous mineralogy and in places the description of texture is difficult. Pieces were recovered that display primary igneous textures and layering and secondary ductile fabrics. Alteration appears to have caused static replacement of the primary igneous phases in places, forming pseudomorphs after olivine in a similar manner to that observed in Site 922 gabbroic rocks (Fig. 5; see "Metamorphic Petrology" section, "Site 922" chapter, this volume).

Olivine gabbro is typically medium- to coarse-grained and displays a range of textures from coarse-grained inequigranular to poikilitic. The maximum range of grain sizes is constrained principally

by the presence or absence of poikilitic clinopyroxene and olivine. Olivine ranges from 3% to 35% in modal abundance, clinopyroxene from 5% to 38%, and plagioclase from 50% to 70%. A conspicuous feature of these rocks is that olivine is almost always a cumulus phase, as is plagioclase.

Fine-scale (2–5 cm) layering is defined by variations in the modal abundances of olivine and plagioclase, producing interlayered sequences of plagioclase-rich and plagioclase-poor troctolite (Figs. 6, 7, and 8). Olivine gabbro occurs where sporadic clinopyroxene oikocrysts develop (Fig. 9). This layering has a moderate dip throughout Holes 924B and 924C. Olivine is typically subhedral and cumulus (Fig. 7) and in places is crescumulus. As in other sites, clinopyroxene is typically green where oikocrystic and brown where it appears as an abundant primocryst phase.

Modal layering of plagioclase and olivine is sporadically overgrown by large poikilitic green clinopyroxene grains (Fig. 6). The oikocrysts are typically not abundant, but they range up to 80 mm in diameter. The effect of this distribution is to produce an interlayering of olivine gabbro and troctolite (e.g., Section 153-924C-6R-1). At one occurrence, a pegmatitic layer of olivine gabbro occurs within a medium-grained olivine gabbro. The maximum grain size of clinopyroxene and olivine in these layers is 5 cm and 1.5 cm, respectively. The clinopyroxene crystals have large inclusion-free cores, but they subophitically enclose plagioclase in their margins (Fig. 6).

In Section 153-924B-2R-1 (Piece 1), fine-scale modal layering is present as subvertical, undulating layers of fine-grained gabbro, poikilitic olivine gabbro, and troctolite. The poikilitic olivine gabbro typically contains green clinopyroxene, but where adjacent to the contact with gabbro, brown clinopyroxene occurs. Gabbroic rocks underlying this sample (Section 153-924B-3R-1) are undeformed and clinopyroxene forms both euhedral, brown cumulus grains and zoned, green poikilitic grains with brown rims.

The best developed occurrence of modal and grain-size layering is within a 1- to 2-m-thick interval in Sections 153-924C-5R-1 and 5R-2. The sequence in this core grades downward from poikilitic olivine gabbro containing scattered large, clinopyroxene oikocrysts into very coarse-grained troctolite in which both olivine and plagioclase are cumulus phases. Plagioclase grains are highly elongate, and locally they form magmatically aligned clusters with olivine. The scattered clinopyroxene oikocrysts are very coarse-grained, up to the full width of the core, and occupy interstitial spaces as optically continuous crystals. A large clot (6 cm) of very coarse-grained, brown cumulus clinopyroxene associated with iron oxide minerals occurs within this interval. The base of the coarse-grained interval was not recovered, but the underlying piece is medium-grained and shows a fine-scale modal layering. Large clinopyroxene oikocrysts are present within the underlying rocks as overgrowths on crescumulus olivine dendrites. Fine (2–5 cm) modal layering continues in troctolite and olivine gabbro to the end of the core.

### Downhole Variations

The rocks from Hole 924B contain 57% ± 5% plagioclase, 25% ± 10% clinopyroxene, and 17% ± 8% olivine (Fig. 10). Rocks from Hole 924C contain 61% ± 8% plagioclase, 12% ± 9% clinopyroxene,

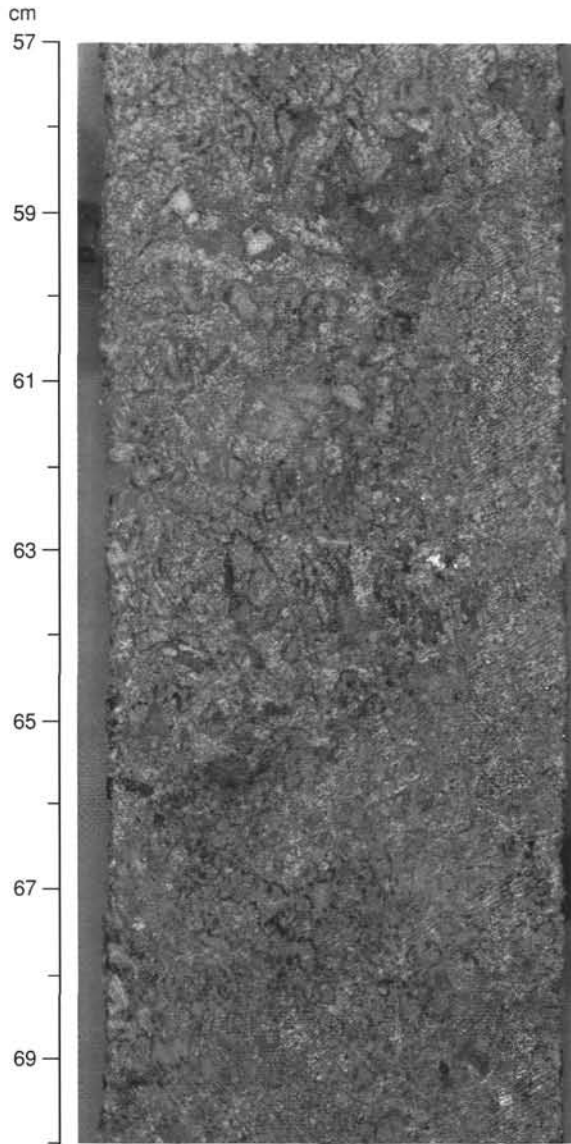


Figure 5. Sample 153-924C-2R-2, 57–70 cm, showing olivine pseudomorphs rimmed by dark coronas of chlorite. Poikilitic clinopyroxene appears as the uniformly dark mineral.

and  $27\% \pm 7\%$  olivine. Although only a limited amount of core was recovered from Hole 924B, it is clear that the rocks from Hole 924C are more olivine rich and have more variable clinopyroxene abundances than those from Hole 924B.

Little can be said about the vertical sequence of rock types encountered in Hole 924B because drilling difficulties may have resulted in a repetition of the rock sequence beginning with Core 153-924B-4W. However, Hole 924C was drilled to a depth of 48.5 m with a cumulative recovery of 23.1%. In rocks from Hole 924C, the abundance of olivine typically ranges from 20% to 30%, but shows no systematic variation with depth or with respect to clinopyroxene abundance (Fig. 10). In contrast, plagioclase varies from 60% to 70% at the bottom of Hole 924C to approximately 50% at the top. Clinopyroxene is typically present in abundances of less than 10% below 30 m depth, but varies erratically in the upper 30 m of the hole where it forms up to 35% of the rock. Although clinopyroxene is clearly more abundant in the upper 30 m of Hole 924C, the erratic distribution of modal abundance shown on the downhole plot is a function of the heterogeneity in the distribution of the clinopyroxene oikocrysts combined with limitations in the way the data are averaged over the length of a piece.

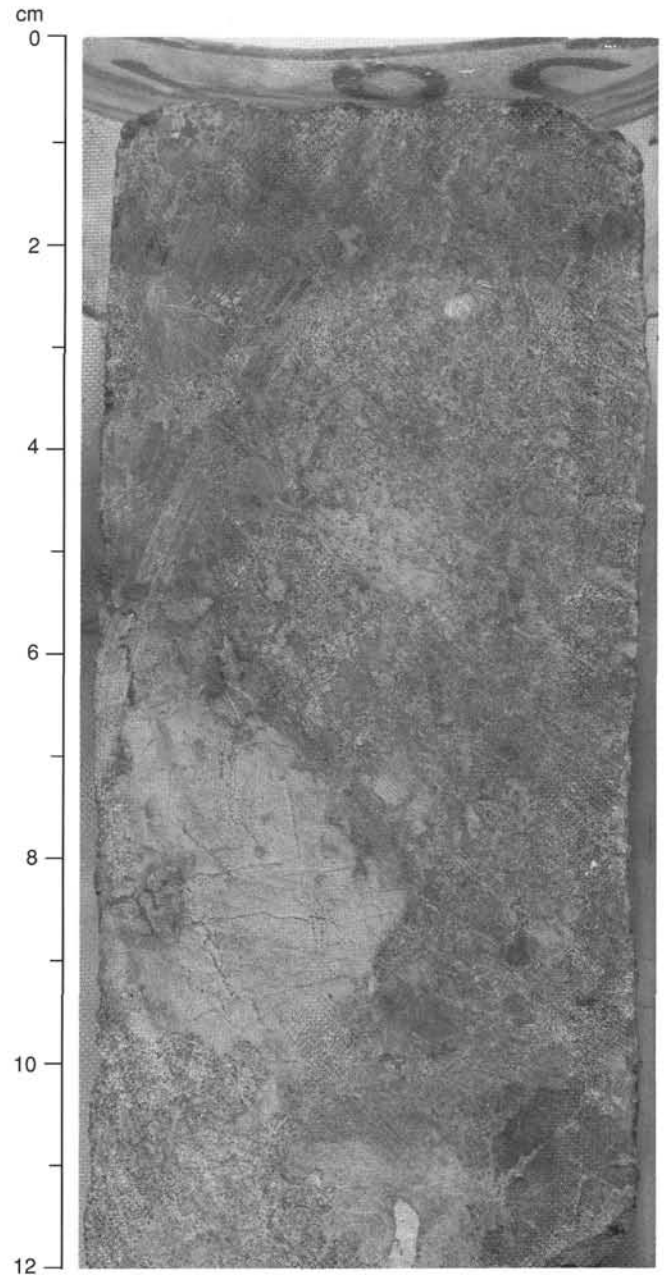


Figure 6. Sample 153-924C-2R-1, 0–12 cm, showing a coarse-grained to pegmatitic layer of olivine gabbro adjacent to a fine- to medium-grained olivine gabbro. The large clinopyroxene crystal has an inclusion-free core but subophitically encloses plagioclase along its boundaries (white tabular grain in clinopyroxene between 11 and 12 cm in the photograph). Olivine occurs as the dark anhedral crystal on the edge of the core between 10 and 12 cm in the photograph.

## Discussion

Site 924 samples include lineated gabbro, olivine gabbro, poikilitic olivine gabbro, and troctolite. Holes 924B and 924C are similar to each other in consisting predominantly of olivine gabbro and troctolite, but Hole 924B contains a significant proportion of lineated gabbro. Given the gross similarity in rock types, the rocks recovered from Holes 924B and 924D are somewhat lithologically distinct from other sites drilled during Leg 153. The predominance of olivine gabbro and troctolite distinguishes these rocks from those recovered at Sites 921 and 923, which are dominated by gabbro and olivine-poor olivine gabbro. Site 924 mafic rocks are most similar to those from

Site 922, but oxide gabbros and other evolved compositions are absent. Despite the relatively high degree of alteration, the olivine-rich gabbroic rocks from Site 924 exhibit a very similar range in mesoscopic magmatic textures to those of olivine gabbro recovered from Hole 923A. They resemble rocks from Site 922, however, in terms of the alteration style.

The Site 924 gabbroic rocks are, nonetheless, distinct from other sites in two aspects. The first is that olivine gabbro contains both oikocrystic green clinopyroxene and interstitial to cumulus brown clinopyroxene in the same samples. Although it was suggested that some of the contacts between gabbro and poikilitic gabbro in rocks recovered from Site 921 may be gradational (see "Igneous Petrology" section, "Site 921" chapter, this volume) in no case was there a clear association of poikilitic green clinopyroxene and cumulus brown clinopyroxene observed in the same sample. In contrast, the relationship between the two types of clinopyroxene grains occurring in the Site 924 rocks (particularly within Section 153-924B-3R-1) suggests that some of the gabbro recovered from Site 924 may be transitional in chemistry between poikilitic olivine gabbro and brown clinopyroxene gabbro. The second observed difference between the rocks sampled from Site 924 and those from Site 921 and 923 is in the predominance of olivine-rich gabbroic rocks (Site 924) over brown clinopyroxene-bearing gabbroic rocks (Sites 921 and 923). Nonetheless, the macroscopic textures of troctolitic gabbro from Site 924 are similar to those from Sites 922 and 923, where olivine-rich rocks comprise almost half of the suite of rocks. These observations suggest that the gabbro massif drilled at Site 921 to Site 924 is heterogeneous in composition on both centimeter- to meter-scales. This is evident from the variations within rocks sampled from individual holes and between closely spaced drill holes such as at Site 922 and Site 924. It is also apparent that there is a larger scale heterogeneity (hundreds of meters), as is evident from the variations between individual sites.

### METAMORPHIC PETROLOGY

Gabbroic rocks recovered from Holes 924B and 924C show variable degrees of alteration (5%–80%). Alteration of gabbro, poikilitic gabbro, olivine gabbro, and troctolite at Site 924 is dominated by static metamorphism that commonly obscures primary magmatic textures and mineralogy. Primary minerals are commonly replaced by actinolite-tremolite, talc, chlorite, smectite, and oxide and sulfide minerals. Brown amphibole, secondary plagioclase, and prehnite are less abundant. Alteration intensity and style are similar to Site 922, though hydrothermal veins are generally finer and less abundant than in gabbroic rocks from Site 922. Porphyroclastic textures and domains of neoblasts indicative of dynamic recrystallization are locally present in lineated gabbro intervals.

The following sections describe the alteration of primary minerals and the vein mineralogy from rocks sampled at Site 924. This description is based only on macroscopic observations; this site was not sampled for thin sections because of time constraints at the end of the leg.

#### Alteration of Primary Phases

Rock types recovered at Site 924 include variably deformed gabbro, olivine gabbro, and troctolite (see "Igneous Petrology," this chapter) that exhibit variable intensities of both dynamic metamorphic effects and static hydrothermal alteration (Fig. 11), as well as minor veining. Alteration features are described below, but detailed characterization of textural relationships will require shore-based investigation.

#### Olivine

In the gabbroic rocks, olivine records variable alteration intensities, from slight to pervasive (5% to 100%; See Fig. 7) and is characterized by well-developed coronitic rims. In the least altered grains, fresh kernels of olivine are cut by microfractures containing oxide minerals, and are rimmed by brown-yellow smectite and/or talc.

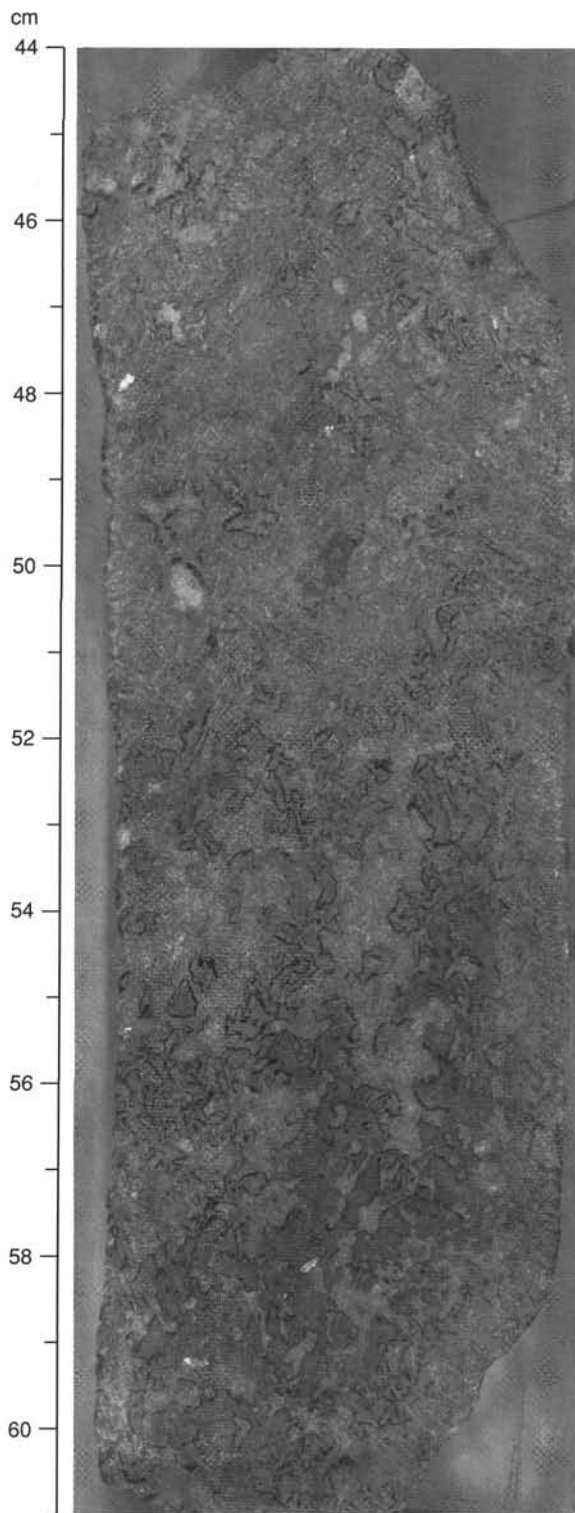


Figure 7. Sample 153-924C-1R-1, 44–61 cm, showing olivine pseudomorphs rimmed by dark chlorite coronas and modal layering between olivine gabbro at the bottom of the piece and troctolite at the top.

In troctolitic gabbros fresh kernels of olivine are enclosed by complex intergrowths of smectite, chlorite, and actinolite, which form amoeboid pods (Fig. 7). Pervasive replacement of olivine by talc or smectite and oxide minerals is more common in troctolite than in rocks with less olivine.

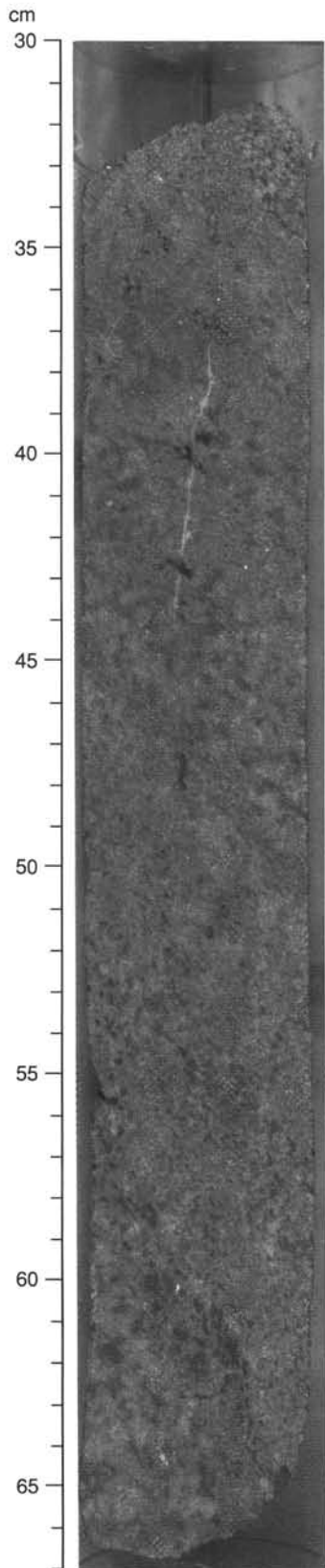


Figure 8. Sample 153-924C-6R-1, 30–67 cm, showing inclined modal layering in troctolite defined by variations in the modal proportions of olivine to plagioclase.

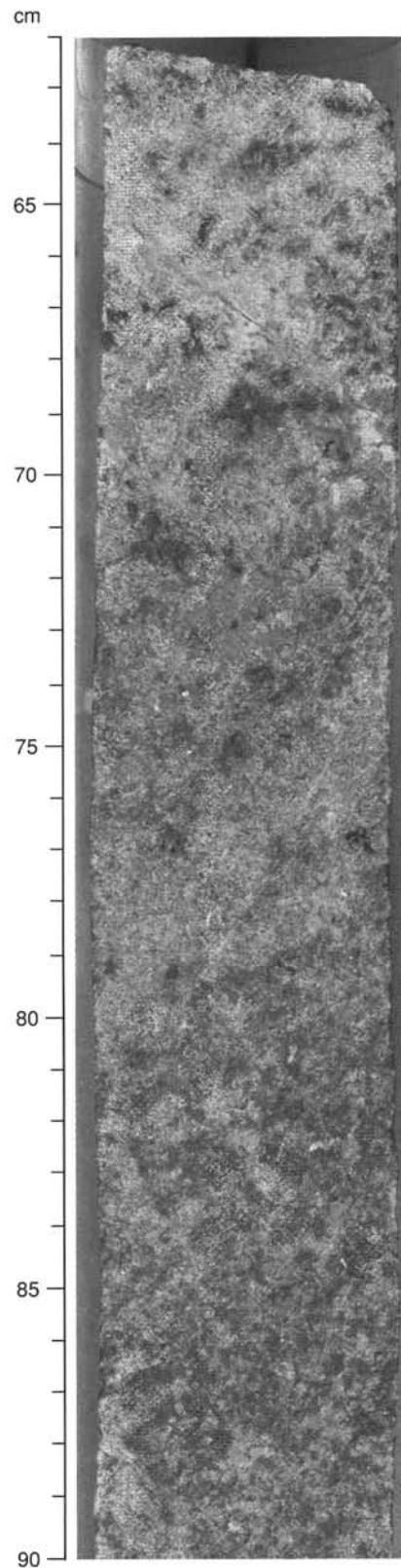


Figure 9. Sample 153-924C-3R-1, 62–90 cm, showing diffuse modal layering from (bottom to top): medium-grained troctolite, medium-grained anorthositic troctolite, coarse-grained olivine gabbro, and medium- to coarse-grained troctolite. Note gradational nature of layer contacts.

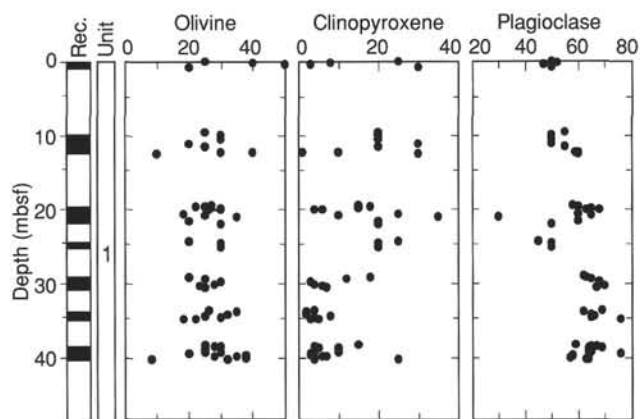


Figure 10. Downhole variations in visually estimated modal abundances of olivine, clinopyroxene, and plagioclase in Hole 924C.

In highly altered olivine gabbro, olivine exhibits well-developed coronas (Section 153-924B-4W-1, Piece 5B) composed of coarse-grained olivine cores that are partially replaced by talc and oxide minerals. They are concentrically rimmed by fibrous amphibole and talc. The outermost rim is composed of dark green chlorite. Coronitic replacement is widespread in most of the olivine gabbro recovered. Alteration of olivine is commonly intense near chlorite-filled veins.

#### Clinopyroxene

Clinopyroxene is variably altered, and, like olivine, grains exhibit well developed coronitic textures. Brown amphibole after clinopyroxene is commonly present as inclusions and as discontinuous rims around the grains. In deformed intervals, the coarse pyroxene grains are elongated. Small grains of neoblastic clinopyroxene and minor amounts of brown amphibole are present in tails of stretched clinopyroxenes (Section 153-924B-4W-1, Piece 5A). Randomly oriented fibrous actinolite, in turn, encloses the smaller grains within the tails and represents a static overprint. Textures suggest that crystal-plastic deformation of clinopyroxene occurred in amphibolite facies, whereas alteration continued to greenschist facies conditions.

In more pervasively altered samples, clinopyroxene is partially or totally replaced by pale green to green actinolite-tremolite (Section 153-924C-2R-2, Pieces 1–2). Where clinopyroxene is completely replaced by actinolite-tremolite, a dark green rim of chlorite bounds these minerals and adjacent plagioclase. In the most altered rocks, the cores of clinopyroxene grains are locally replaced by white-yellow tremolite and probable clay minerals and are rimmed by chlorite zones that can reach 1 to 2 mm in width. Coarse-grained, light green oikocrysts of clinopyroxene in poikilitic gabbro are pervasively replaced by very fine-grained fibrous actinolite-tremolite.

#### Plagioclase

Alteration of plagioclase ranges from negligible to pervasive. Secondary phases include clay minerals and chlorite, secondary plagioclase, and minor prehnite (Section 153-924C-2R-2). Alteration of plagioclase commonly varies within a single section. Grains are commonly cut and rimmed by chlorite and chlorite + actinolite veinlets. Irregular patches of secondary plagioclase occur in alteration halos near veins (Section 153-924C-7R-1, Piece 15).

#### Mineralogy of Hydrothermal Veins

Actinolite + chlorite-filled veins are the earliest vein set in both Holes 924B and 924C. The dark green veins range in width from 1 to 5 mm. Wall-rock alteration is intense adjacent to these veins, and is characterized by chlorite, actinolite, and secondary plagioclase (Fig.

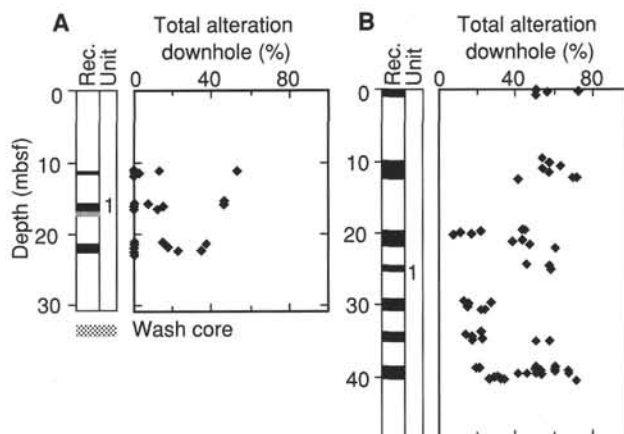


Figure 11. **A.** Downhole variation of alteration in gabbroic rocks from Hole 924B, macroscopic visual estimates of alteration of the primary phases. **B.** Downhole variation of alteration in gabbroic rocks from Hole 924C, macroscopic visual estimates of alteration of the primary phases.

12). Composite veins with chlorite margins and pale green smectite cores are also present at Site 924 and represent a third generation and late set of veins.

In Section 153-924C-2R-1 (Piece 1B), an irregular millimeter- to centimeter-sized prehnite- and epidote-filled vein is present. Globular clusters of radiating fibers (up to 1.5 mm in diameter) of milky white prehnite are associated with submillimeter-sized epidote grains. The prehnite and epidote vein in this sample is cut by a thin (<1 mm) actinolite-filled vein and thus appears to represent an earlier type of vein.

#### Downhole and Cross-hole Variation in Alteration

The plot of Figure 11 shows no systematic change in the intensity of alteration downhole at Site 924. No difference in secondary mineralogy has been noted between the two holes. Alteration in rocks recovered from both holes at Site 924 is generally higher than in rocks from Site 921, though it is comparable to that of rocks from Site 922 (see "Metamorphic Petrology," "Site 922" chapter, this volume).

#### Summary and Discussion

The early stages of metamorphism in gabbroic rocks at Site 924 are marked by dynamic recrystallization of clinopyroxene grains and synkinematic growth of brown amphibole, which likely indicate that deformation occurred at minimum temperatures of 700°–900°C (Spear, 1981; Liou et al., 1974).

Subsequent static alteration of the gabbroic rocks is generally marked by moderate to high intensities that overprint the crystal-plastic deformational fabrics. The earliest static alteration involved limited formation of brown amphibole as rims around olivine and clinopyroxene and as blebs within clinopyroxene. Replacement of olivine, clinopyroxene, and plagioclase by tremolite-actinolite and chlorite indicates that the general background alteration occurred largely under greenschist facies conditions. The close association of these lower temperature phases with vein networks of actinolite and chlorite is consistent with brittle failure and circulation of fluids at temperatures of 300°–450°C.

#### STRUCTURAL GEOLOGY

Drilling at Site 924 resulted in the recovery of variably deformed, fine- to coarse-grained gabbroic rocks that show heterogeneous and commonly extensive alteration. In general, the altered gabbroic rocks from this site are only weakly deformed and display locally devel-

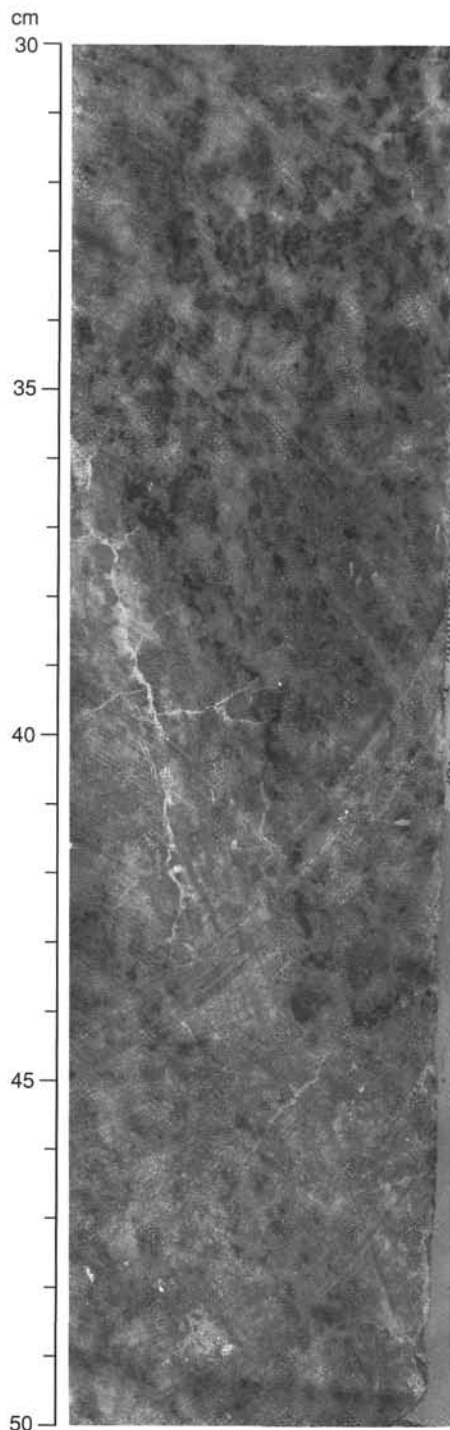


Figure 12. Actinolite-filled vein (cutting core diagonally, left to right from 36 to 49 cm) in troctolite. Note the alteration halo marked by replacement of plagioclase by secondary plagioclase and clinopyroxene by actinolite (Sample 153-924C-3R-1, Piece 5, 30–50 cm).

oped foliation and/or lineation defined by shape preferred orientation of olivine, clinopyroxene, and plagioclase grains, discrete zones of densely spaced fractures, microfractures, and veins and vein arrays, and several discrete faults. The distribution of these structures throughout the core is heterogeneous and does not appear to be related to alteration or inferred igneous protoliths. Magmatic foliation, defined by a preferred orientation of plagioclase laths, is nearly absent. The number of different vein generations is much smaller in rocks

from Site 924 compared to the rocks from Sites 921, 922, and 923. The early felsic veins that were observed in the rocks from other sites are also absent.

### Magmatic Fabrics

Most of the rocks recovered at Site 924 display primary igneous textures despite widespread and pervasive alteration. The most common primary igneous texture in medium- to coarse-grained gabbros is characterized by random orientation of subhedral to anhedral mineral phases with little or no sign of intracrystalline strain. In the olivine-poor gabbros, plagioclase and clinopyroxene are commonly equigranular. In the olivine-rich rocks, clinopyroxene occurs as large (up to several centimeters) oikocrysts. In some places, olivine-rich bands alternating with olivine-poor bands define a compositional layering, which generally has a subhorizontal orientation (Section 153-924C-3R-1, Piece 7). Magmatic foliation is, in general, poorly developed in Site 924 gabbros. Locally, however, a well-preserved magmatic foliation, defined by the preferred orientation of tabular plagioclase crystals and in some cases parallel to layering, is present (e.g., Sections 153-924C-5R-1, Piece 3, and 2R-2, Piece 10).

### Crystal-plastic Fabrics

Mesoscopic crystal-plastic fabrics are characterized by an elongated equigranular texture in fine- to medium-grained gabbroic rocks and an elongated porphyroclastic texture in medium- to coarse-grained rocks. Sugary textured plagioclase is the main constituent of the fine-grained matrix. Medium- to fine-grained gabbros are more extensively affected by crystal-plastic deformation than the coarse-grained ones, and the orientations of foliations and lineations defined by shape preferred orientation of olivine, clinopyroxene, and plagioclase are generally steep to subvertical (Fig. 13). In Sample 153-924C-6R-1 (Piece 2, 30–67 cm) the foliation dips  $57^\circ$  and is oblique to the more steeply dipping diffuse boundaries of modal layering in altered olivine gabbro and troctolite (Fig. 8).

Crystal-plastic fabrics are heterogeneously distributed throughout the core in both Holes 924B and 924C. In a given section, it is common to find one or two pieces showing a well-developed crystal-plastic fabric, whereas all the other pieces lack such features (Sections 153-924C-7R-1, Piece 13, and 6R-1, Piece 2). Sections 153-924C-2R-1 (Piece 3) and 924B-2R-1 (Piece 1) have a sharp boundary between deformed olivine-rich gabbro and undeformed poikilitic gabbro that dips steeply ( $60^\circ$ ). The foliation in these pieces is defined by the preferred shape orientation of elongated olivine grains.

The upper three sections of core in Hole 924B do not, in general, display a crystal-plastic fabric, with the exception of Piece 1 in Section 2R-1 in which elongated olivine grains display a steeply plunging lineation. Piece 5 of Section 4W-1 has a moderately developed shape preferred orientation defined by elongated, coarse pyroxene grains. The foliation plane dips  $50^\circ$  near the top of the piece and becomes shallower ( $35^\circ$ ) near the bottom. Pieces 4, 5, 7, and 13 in Section 5R-1 show a well-developed foliation that is locally parallel to compositional banding (in Piece 4).

In Hole 924C, gabbros in Section 153-924C-1R-1 are weakly but penetratively deformed. Clinopyroxene grains show a shape-preferred orientation, have stretched tails, and are commonly rimmed by green chlorite and in places by actinolite. In Section 2R-1 the rocks are undeformed, except in Piece 3B in which a weak alignment of altered plagioclase grains defines a moderately dipping foliation. Sections 2R-2, 3R-2, 5R-1, and 7R-2 also contain undeformed gabbros. Similarly, Sections 3R-1, 4R-1, and 5R-2 contain undeformed gabbros as well, but some isolated pieces display a weak shape fabric defined by elongated olivine grains. In Piece 6 of Section 4R-1 the elongated clinopyroxene crystals show a lineation plunging steeply ( $75^\circ$ ). In Section 6R-1 (Piece 2), alternation of weakly deformed and strongly deformed bands occurs at a decimeter scale. Elongation and shape preferred orientation of olivine and pyroxene grains form a

moderately to well-developed and steeply dipping ( $50^{\circ}$ – $60^{\circ}$ ) foliation in Pieces 2, 13, 14, and 15 in Section 7R-1.

### Brittle Features

Discrete brittle structures that preserve kinematic indicators are comparatively rare in both Holes 924B and 924C. The structures are limited to minor cataclastic zones, discrete veins and fractures, and minor faults.

### Faults and Joints

A discrete fault is found in Piece 7 of Section 153-924C-6R-1, where a 1-mm-wide moderately dipping fault transects the upper part of the piece. The fault plane contains oblique actinolite and tremolite fibers, suggesting a normal shear sense. Other structures that do not preserve kinematic indicators, but may represent minor faults, include veins containing chlorite and actinolite fibers oriented obliquely to the vein margins (Section 153-924C-3R-1, Piece 6). These veins commonly dip about  $60^{\circ}$ . Chlorite and actinolite veins (1–2 mm wide, similar to those observed at Sites 921, 922, and 923) also form dense arrays, heterogeneously distributed through the core, commonly at the top or the base of the pieces. This suggests that densely fractured or cataclastic intervals between the pieces recovered may have been lost or preferentially excluded during coring. In some cases, slickenside lineations were measured in these veins (e.g., Section 153-924C-3R-1, Piece 5). Some of these swarms contain veins with en-echelon segments (e.g., Section 153-924C-5R-1, Piece 3).

Striations defined by fine grooves are evident on the tops and bases of some pieces. It is unclear whether these structures relate to drilling induced deformation or fault slip. Several minor joints also dissect the core pieces of Hole 924C. Most of the joints have formed along vein surfaces where chlorite and actinolite are present and have a range in dip variations similar to that of the veins.

### Cataclastic Zones

A few intervals of core from Hole 924C contain zones of grain-size reduction, spatially associated with alteration phases and microfractures. During core description these zones were described as cataclastic shear zones although none of these zones contains unambiguous evidence for fracturing and frictional sliding. The best example occurs in Section 2R-1 (Piece 6), where there is a 7-mm-thick, subhorizontal interval where the gabbro is strongly fractured and replaced by actinolite, chlorite, and a yellow clay mineral (Fig. 14). The actinolite needles are oriented obliquely and at a high angle to the vein margins. Dense chlorite and actinolite veins ( $<0.2$  mm) pervade the gabbro in a 2-cm-wide zone surrounding the central alteration zone. The lower zone contains intensely microfractured plagioclase grains in a medium-grained, plagioclase-rich band (Fig. 14). The chlorite and actinolite veins dissect the plagioclase grains in this outer, fractured zone, but the grains do not appear to have been displaced. A less extensively altered zone with weak cataclasis is present in the lower and upper margins of Pieces 4 and 5 of Section 3R-1. These zones also are characterized by a high density of subparallel microfractures within a roughly planar, 0.5-cm-wide zone, dipping at about  $50^{\circ}$ . Some minor cataclasticites with intragranular fractures in pyroxene grains also occur in the upper part of Piece 3 (Section 5R-1), and distributed fracture networks filled with clay minerals are present in Sections 7R-1 (Pieces 5 and 6) and 7R-2 (Piece 6).

### Veins

In gabbroic rocks from both holes drilled at Site 924, veins represent a significant component of brittle deformation; they postdate earlier magmatic and crystal-plastic fabrics. The two main types of veins in Site 924 rocks include chlorite actinolite veins, and veins with various clay and iron oxide minerals. In general, chlorite + actinolite veins represent relatively older veins, whereas those con-

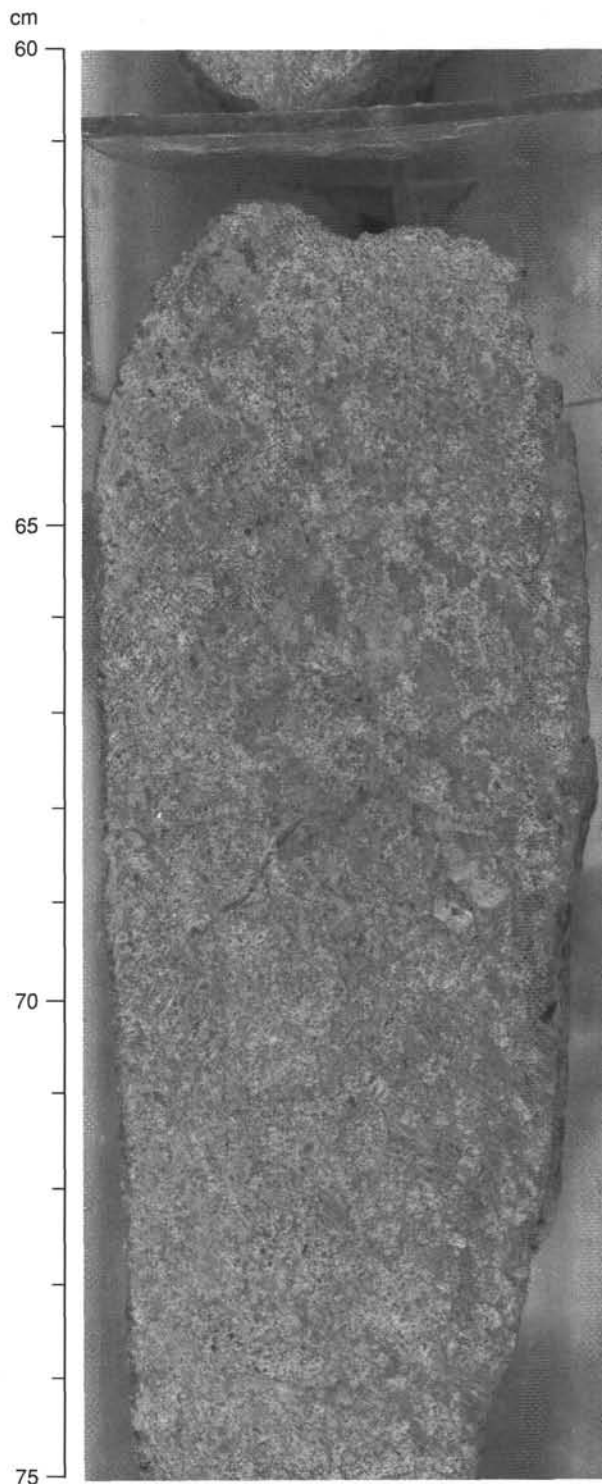


Figure 13. Sample 153-924C-4R-1 (Piece 6, 60–75 cm). Elongated pyroxene porphyroclasts in a pyroxene-rich interval define a strong, steeply plunging ( $75^{\circ}$ ) lineation in a highly altered medium-grained gabbro.

taining clay and iron oxide minerals form younger ones on the basis of crosscutting relations.

### Chlorite + Actinolite Veins

These veins commonly have planar geometry with steep boundaries and include halos and/or zones of alteration in the host rock

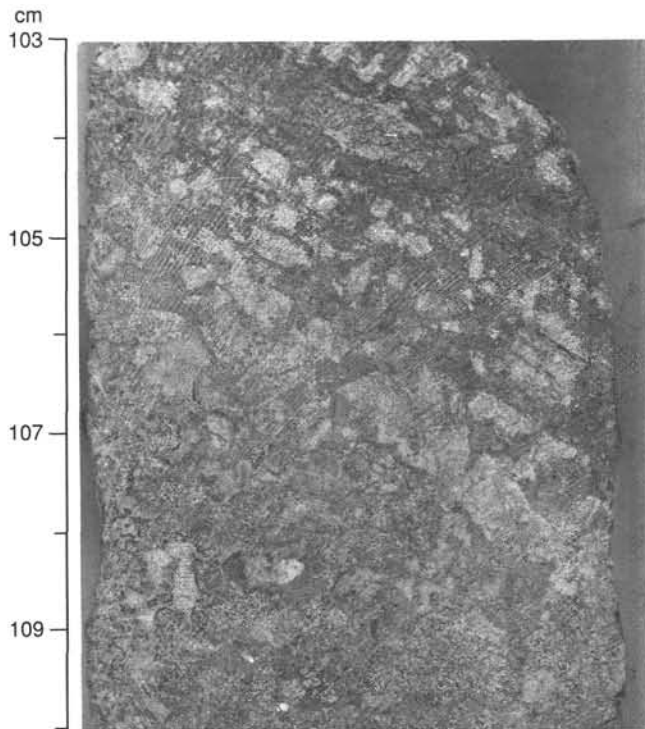


Figure 14. Sample 153-924C-2R-1 (Piece 6, 103–110 cm). A 1-cm-wide zone of reduced grain size in gabbro (intersects right-hand edge of core at 105 cm) is overgrown by chlorite, actinolite, and minor clay minerals. The actinolite has grown obliquely and at a high angle to the margin of the vein, but shows no strong shape preferred orientation. The plagioclase-rich interval (below) is dissected by several thin (<0.5 mm) chlorite and actinolite veins. No offsets are evident across these veins.

immediately adjacent to their margins. The width of the veins varies from less than 1 mm to 10 mm, and their orientations range from subhorizontal to subvertical. They cut across the compositional and textural boundaries and the crystal-plastic fabric elements at oblique to high angles.

The chlorite + actinolite veins locally consist of distributed vein networks and vein arrays. One example was described above in association with a cataclastic zone. Similarly, a 2-mm-wide chlorite + actinolite vein cuts the troctolite in Section 153-924C-3R-1 (Piece 5) and dips steeply ( $66^\circ$ ), parallel to the fabric defined by the weakly elongated and aligned olivine grains. Altered plagioclase forms an irregular patch around this vein. A 30-mm-wide zone of densely spaced, thin, and subparallel chlorite veins occurs adjacent to this chlorite + actinolite vein and forms a vein network in the rock. Discrete but irregular, thin veins (<1 mm wide) containing iron oxide and clay minerals cut across the chlorite + actinolite vein and the adjacent vein network at  $80^\circ$ . In Section 153-924C-7R-1 (Piece 6) chlorite + actinolite veins form a 30-mm-wide zone of vein network in which the plagioclase grains are dissected by numerous subparallel microveins.

An actinolite + chlorite vein in Section 153-924C-6R-1 (Piece 7) crosscuts a 5-mm-wide and steeply dipping shear zone on the back surface of the core and is in turn cut by an irregular vein composed of clay minerals and epidote. The orientation of the mineral fibers within the fault plane suggests a normal sense of shearing along the fault.

#### *Veins with Clay Minerals*

These veins are more common than the previously described group, they are more irregular in their morphology and distribution than the chlorite + actinolite veins, and they commonly contain chlorite and/or iron oxide  $\pm$  prehnite  $\pm$  talc in addition to the clay minerals.

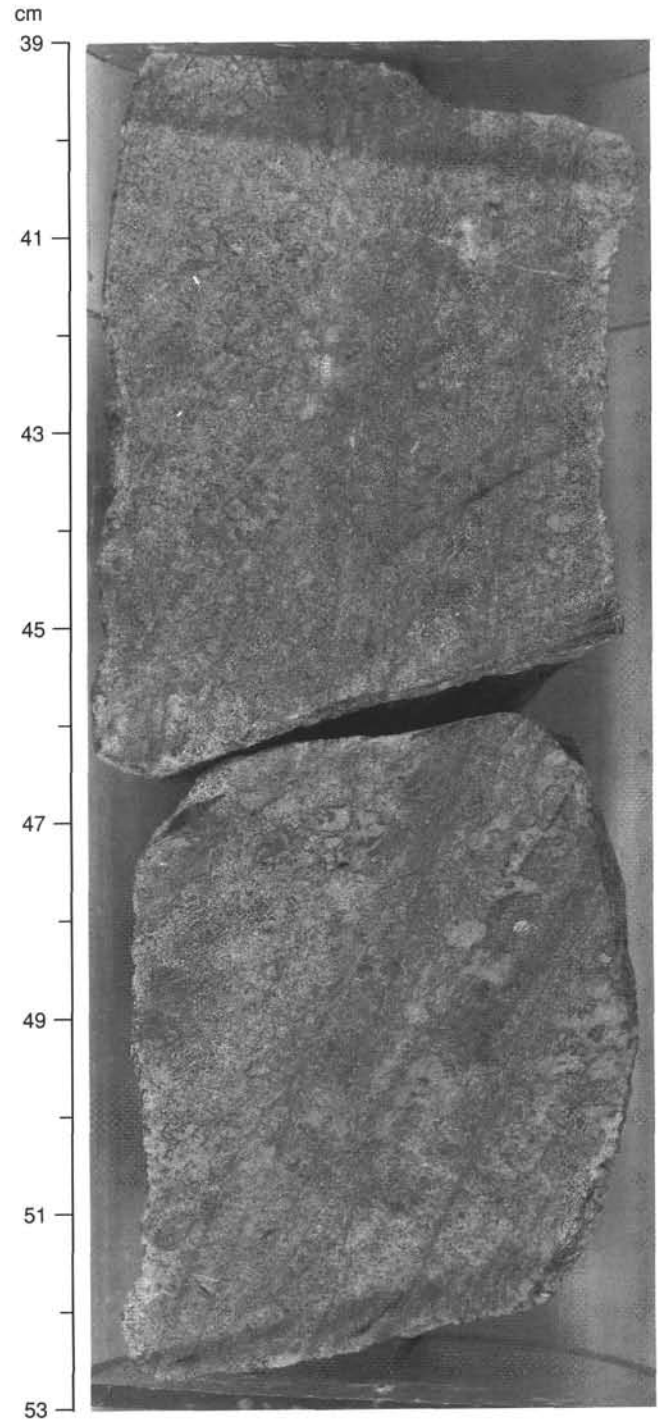


Figure 15. Sample 153-924C-7R-1 (Piece 6, 39–53 cm). A dense array of steeply dipping chlorite + actinolite veins cuts through plagioclase grains but does not displace them. The veins are hosted by a strongly altered medium- to coarse-grained olivine gabbro and are cut by white veins of clay minerals at 41.5 cm.

They are generally thin (<1 mm) and form individual veins and/or vein networks. They locally display en-echelon and overlapping segments and in some cases change their mineralogy along their traces depending on the mineral composition of the host rock (e.g., Section 153-924C-6R-1, Piece 2). In some cases, the dip of individual, continuous veins changes from subhorizontal to subvertical. They overprint other structures and the chlorite + actinolite veins. A swarm of shallow-dipping chlorite and actinolite veins is concentrated in a

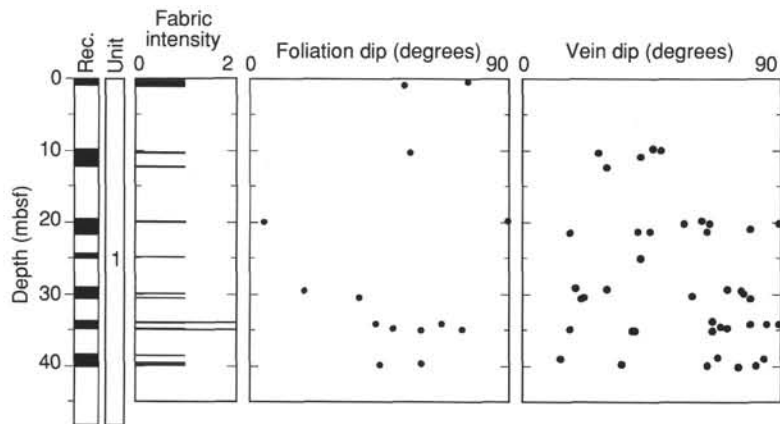


Figure 16. Composite plot of foliation intensity, foliation dip, and vein dip for Hole 924C. Although some kinds of foliation measurements were recorded, true dips could not be determined in all cases. All cores contain pieces with at least a weak preferred mineral alignment. Core 924C-6R contained the only pieces with moderate shape preferred orientation (intensity 2). These moderate-intensity foliations dip  $45^{\circ}$ – $80^{\circ}$ .

1-cm-wide zone in Sample 153-924C-7R-1, 39–53 cm, cut by steeply dipping veins of white clay minerals (Fig. 15).

Many of the veins with clay and oxide minerals form dense vein arrays and networks contributing to the total alteration in the gabbroic rocks. Some vein arrays occur within individual plagioclase and clinopyroxene grains (e.g., Sections 153-924B-4W-1, 2R-1, and 3R-1). Felsic veins and epidote-bearing veins common to gabbroic rocks from Sites 921, 922, and 923 do not occur in the gabbroic rocks from Site 924.

### Downhole Variations and Discussion

All cores contain at least a weak shape preferred orientation. Only near the base of the core, in Core 924C-6R, is a moderately strong crystal-plastic fabric developed (Fig. 16). In general, the foliation and lineation dip moderately to steeply. In a few sections the foliation changes from a steeply dipping into a subhorizontal orientation (923C-1R-1).

No veins were measured at the top of Hole 924C in Core 1R (Fig. 16). The remainder of the cores contained veins with a wide variation in dip, from subhorizontal to vertical. Veins are commonly single and thin, or they occur as a closely spaced set of very thin (<1 mm) parallel microveins making up a composite vein. Both crosscutting veins and sets of parallel veins, other than composite veins, are rare.

### PALEOMAGNETISM

Site 924 is located approximately 1.7 km east of Sites 921 and 923, which were both characterized by predominantly reversed polarity magnetizations. Samples from Site 924 were used to evaluate whether normal polarity gabbroic rocks outcrop closer to the median valley axis than at Sites 921 and 923.

### Whole-core and Half-core Measurements

Susceptibility measurements for Site 924 gabbros span two orders of magnitude, from  $5 \times 10^{-4}$  to  $5 \times 10^{-2}$  SI. Alteration of olivine to talc, smectite, chlorite, and magnetite (see "Metamorphic Petrology," this chapter) is well developed in many intervals within the core. Intervals with abundant, altered olivine are associated with high susceptibility values (e.g., the large dendritic olivine in Piece 7, Section 153-924C-1R-1).

The initial intensities of gabbros recovered from Holes 924B and 924C are on the order of 1 to 3 A/m, as indicated by the inability of the cryogenic magnetometer to measure most sections reliably. Half-core measurements from Site 924 show predominantly shallow positive inclinations (typically  $0^{\circ}$ – $30^{\circ}$ ) after demagnetization at 20 mT. There are, however, a few intervals with shallow negative inclinations, for example Hole 924C between 12.25 and 12.45 mbsf (Fig. 17). This figure also shows the values obtained from two discrete samples taken from this core. Demagnetization data from discrete samples corroborate the half-core data, with shallow positive (or less commonly negative) inclinations.

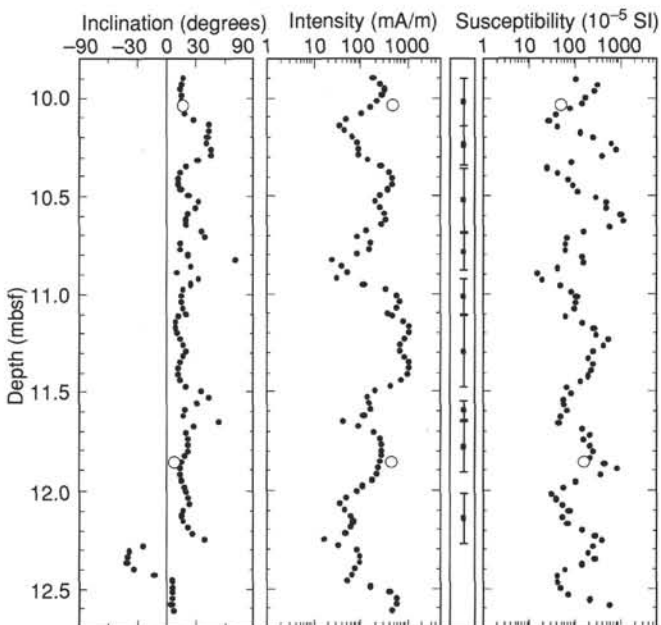


Figure 17. 20 mT inclination and intensity data with initial susceptibilities for Core 153-924C-2R (dots), together with data from two discrete samples taken from the core (open circles). Inclinations downhole are shallow and positive, except in the interval 12.3–12.4 mbsf. The distribution of continuous core pieces longer than 15 cm is shown in the column adjacent to the downhole intensity log.

### Discrete Samples

Natural remanence magnetization and stepwise AF demagnetization measurements were made on selected samples from Site 924 (Table 3). Time constraints at the end of drilling operations precluded detailed sampling of cores from Hole 924C: only five samples were taken from the upper three cores. The NRM intensities of these samples vary greatly, from 0.17 A/m to 20 A/m with a mean of approximately 3 to 4 A/m. One sample in particular has very high NRM intensity of 20 A/m (Sample 153-924C-1R-1, 46–49 cm). This sample was taken within an interval with a large, dendritic olivine (see "Igneous Petrology," this chapter), the alteration of which may account for the high susceptibility and remanent magnetization of this sample. Initial susceptibilities range from a high of 0.06 SI to a low of 0.0005 SI, generally corresponding to the relative highs and lows seen in the intensity measurements.

Demagnetization of discrete samples generally reveals a low-stability, drilling-related remanence that is removed by AF fields of

Table 3. Discrete sample paleomagnetic data from Site 924.

Core, section, interval (cm)	Piece	Depth (mbsf)	NRM			AMS				
			Dec.	Inc.	Int. (A/m)	K (SI)	P	L	F	Q
153-924B-										
3R-1, 88–91	9	16.68	42.9	18.1	4.28	0.01484	1.116	1.040	1.074	9.42
5R-1, 53–56	4	21.83	193.2	-3.2	0.17	0.00093	—	—	—	5.89
153-924C-										
1R-1, 46–49	7	0.46	13.5	81.2	20.08	0.06183	1.123	1.076	1.044	10.61
2R-1, 13–16	2	10.03	214.4	23.9	0.53	0.00057	—	—	—	30.32
2R-1, 75–78	4	11.86	68.4	17.0	0.50	0.00156	1.136	1.080	1.052	10.52
3R-1, 30–33	5	19.90	72.3	72.6	2.75	0.00993	1.120	1.095	1.023	9.05
3R-2, 72–75	4	21.68	292.2	45.4	1.91	0.00221	1.111	1.059	1.049	28.18

Notes: Table includes volume susceptibility ( $K$ ), natural remanent magnetization (NRM), magnetic fabric parameters ( $P = K_1/K_3$ ,  $L = K_1/K_2$ ,  $F = K_2/K_3$ , where  $K_1$ ,  $K_2$ , and  $K_3$  are the maximum, intermediate, and minimum axes of the susceptibility ellipsoid, respectively),  $Q =$  Koenigsberger ratio.

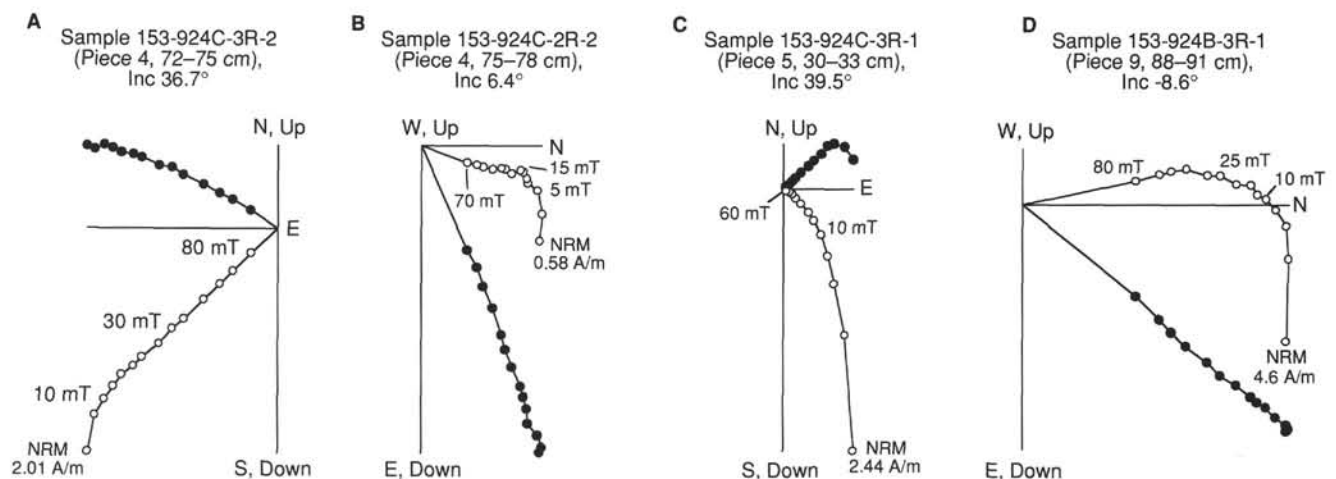


Figure 18. Vector endpoint diagrams for four samples from Site 924. The samples all show varying degrees of drilling induced overprints which are removed by 10 mT. Sample 153-924B-3R-1, 88–91 cm, has a shallow negative final inclination, while the other samples have positive inclinations.

approximately 10 mT or less (Fig. 18). The highest stability components of magnetization generally have positive inclinations ( $20^\circ$  to  $30^\circ$ ), although one sample from Hole 924B has a characteristic remanence with an inclination of  $-8^\circ$  (Fig. 18D). The downward directed, drilling-induced remanence in this sample indicates that the piece has not been misoriented, and the small angular difference ( $\sim 25^\circ$ ) between the characteristic magnetization and the moderate stability ( $< 25$  mT) overprint suggests that this sample is of normal polarity. A second sample from Hole 924B has a steeper negative ( $-28^\circ$ ), high stability magnetization. Although this negative inclination component does not trend toward the origin, its presence suggests that multiple polarities may be present in this location as well as at the other gabbro sites.

## PHYSICAL PROPERTIES

Physical properties measurements were completed on seven samples selected from Holes 924B and 924C. No samples were taken from Hole 924A due to the lack of recovery. Sampling was restricted to the first three of seven cores recovered from Hole 924C, owing to time constraints for analysis and archiving of data prior to port call. The samples were analyzed for horizontal compressional-wave velocity ( $V_p$ ), resistivity, and a determination of index properties (bulk density, grain density, water content, porosity, and dry density; Table 4). Thermal conductivities were determined from four half-round archive sections of core (Table 5). Bulk whole-core densities were

also measured using the gamma-ray attenuation porosity evaluator (GRAPE) component of the multisensor track. However, the limited recovery typical of shallow holes limits utility of GRAPE data (see also "Site 922" chapter, "Physical Properties" section, this volume) and consequently, GRAPE data are not incorporated in this report. Descriptions of experimental methods are provided in the "Physical Properties" section of the "Explanatory Notes" (this volume) and in the "Explanatory Notes" of the Leg 147 *Initial Reports* (Shipboard Scientific Party, 1993).

The following discussion briefly summarizes index properties for this site and considers relationships between various physical properties examined at this and previous sites.

## Data

Bulk densities, porosity, water content, and void ratio were determined (with salt volume corrections for a salinity of 0.032) from wet and dry mass and volume measurements of minicores sampling the olivine gabbro recovered at Site 924. Bulk densities range from 2.82 to 2.92 g/cm<sup>3</sup>, with a median value of 2.86 g/cm<sup>3</sup>. Grain densities are essentially the same as bulk densities, ranging from 2.83 to 2.94 g/cm<sup>3</sup>, with a median value of 2.88 g/cm<sup>3</sup>. This reflects the relatively low porosity (0.38% to 1.04%, median value 0.68%) characteristic of these rocks.  $V_p$  ranges from 5288 to 5755 m/s, with a median value of 5524 m/s. The rocks from Site 924 display thermal conductivities ranging from 2.65 to 3.4 W/m<sup>2</sup>°C, with a median value of 2.9 W/m<sup>2</sup>°C.

**Table 4. Index properties, horizontal compressional-wave velocities ( $V_p$ ), resistivities, and water contents of the crystalline rocks recovered from Site 924.**

Core, section, interval (cm)	Piece	Depth (mbsf)	$V_p$ (m/s)	Resistivity ( $\Omega$ m)	Wet-bulk density ( $g/cm^3$ )	Dry-bulk density ( $g/cm^3$ )	Grain density ( $g/cm^3$ )	Void ratio	Porosity (%)	Water content (%)	Alteration estimate (%)	Rock type	Unit
153-924B-													
3R-1, 88-90	9	16.68	5341	247	2.848	2.842	2.859	0.0059	0.590	0.212	50-70	OG	1
5R-1, 53-55	4B	21.83	5524	256	2.922	2.911	2.942	0.0106	1.044	0.367	25-30	OG	1
153-924C-													
1R-1, 46-48	7	0.46	5755	118	2.907	2.903	2.914	0.0039	0.386	0.136	80	OG	1
2R-1, 13-15	1B	10.03	5531	160	2.841	2.835	2.853	0.0064	0.637	0.230	>20	OG	1
2R-2, 75-77	4	11.86	5443	117	2.861	2.854	2.875	0.0073	0.728	0.261	50-70	OG	1
3R-1, 30-32	5	19.90	5696	87	2.818	2.811	2.830	0.0068	0.676	0.246	40-70	OG	1
3R-2, 72-74	4	21.68	5288	89	2.870	2.862	2.884	0.0076	0.756	0.270	80	OG	1

Notes: OG = olivine gabbro. Unit identification from visual core descriptions.

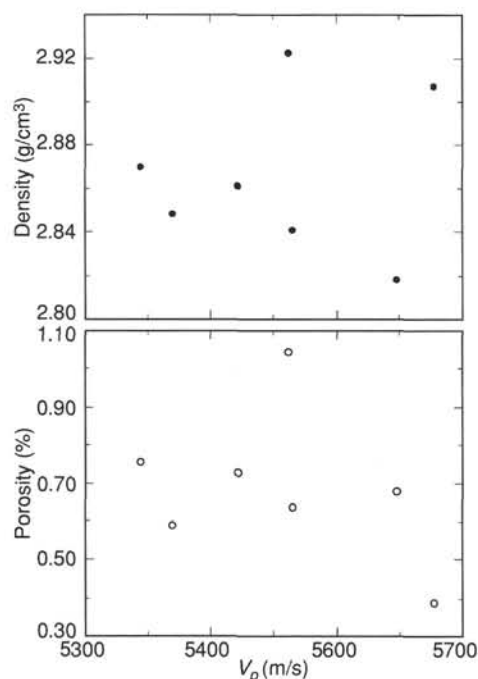


Figure 19. Velocity ( $V_p$ ) vs. density and velocity ( $V_p$ ) vs. porosity for rocks recovered at Site 924.

Compressional-wave velocity ( $V_p$ ) in rocks from Site 924 generally appears to decrease with increasing density (Fig. 19), opposite the trend for crystalline rocks. Velocity also decreases with increasing porosity (Fig. 19) at Site 924, as is generally the case in gabbroic rocks sampled from ocean basins (Christensen, 1982).

### Comparative Analysis of Site 924 Physical Properties Measurements

The physical properties of rocks recovered from Site 924 are almost identical to those obtained from Site 922. Density and velocity are less than were observed in rocks recovered from Sites 921 and 923, and thermal conductivities in rocks recovered from Site 924 (and Site 922) are considerably greater than those observed in rock recovered from Sites 921 and 923. These results are all indicative of comparatively higher extents of alteration in the rocks sampled at Site 924 (and Site 922) than was observed at Sites 921 and 923. The median compressional-wave velocity (5524 m/s) is comparable to that observed in gabbroic rocks with similar densities and low to moderate porosities recovered from fracture zones in the Atlantic (e.g., compilation of Christensen, 1982) but are somewhat less than

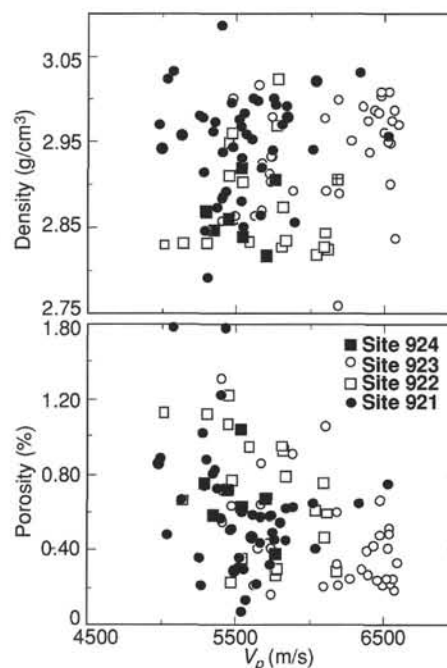


Figure 20. Velocity ( $V_p$ ) vs. density and velocity ( $V_p$ ) vs. porosity for rocks recovered at Sites 924, 923, 922, and 921.

observed in rocks from Hole 735B in the southwest Indian Ocean (Robinson, Von Herzen, et al., 1989) or from the Hess Deep area (Gillis, Mével, Allan, et al., 1993).

The trend of decreasing velocity with increasing density shown in Figure 19 may be due to an increase in high density, low velocity alteration products. However, a greater number of samples is required to establish whether the trend is indeed robust. Site 924 results fall within the widely scattered field of velocity-density observations from Sites 921, 922, and 923 (Fig. 20). The observed decrease in velocity with increasing porosity in rocks recovered at Site 924 follows the general trend observed at Sites 921, 922, and 923 (Fig. 20).

Resistivities measured in gabbroic rock from Site 924 are shown in Figure 21 in terms of the formation factor (ratio of rock and pore water resistivity) and porosity (shown as a ratio of rock volume corrected for salt) together with results from Sites 921, 922, and 923. The data from Site 924 do not form a trend of increasing resistivity with decreasing porosity, as has been observed in gabbroic rocks recovered from Hole 735B (e.g., Pezard et al., 1991). This has been the case for most of the gabbroic samples measured on Leg 153. While some of the scatter may be due to limitations in experimental procedures, downhole changes in resistivity trends have been found

**Table 5. Thermal conductivities for archive half round core pieces and alteration, rock type, and unit identification from visual core descriptions, Site 924.**

Core, section, interval (cm)	Piece	Depth (mbsf)	Thermal conductivity (W/m°C)	Alteration (%)	Rock type	Unit
153-924C-						
1R-1, 43-62	7	0.43	3.410	80	OG	1
2R-1, 25-45	2	10.15	2.649	>20	OG	1
3R-1, 27-50	5	19.87	2.719	40-70	OG	1
3R-2, 61-79	4	21.57	3.064	80	OG	1

Note: OG = olivine gabbro.

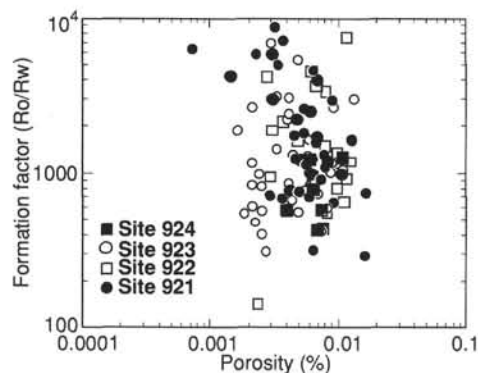


Figure 21. Formation factor (ratio of rock and pore water resistivity) vs. porosity (corrected for salt) for rocks recovered at Sites 924, 923, 922, and 921.

to generally coincide with variations in other observed physical properties (see also "Site 923" chapter, "Physical Properties" section, this volume), perhaps indicating that the mechanisms for electronic conduction in the compositionally and texturally diverse suite of gab-

broic rocks recovered in the MARK area during Leg 153 are themselves variable in nature.

#### REFERENCES\*

- Auzende, J.M., Cannat, M., Gente, P., Henriot, J.P., Juteau, T., Karson, J.A., Lagabrielle, Y., and Tivey, M.A., 1993. Deep layers of mantle and oceanic crust exposed along the southern wall of the Kane Fracture Zone: submersible observations. *C.R. Acad. Sci. Ser. 2*, 317:1641-1648.
- Christensen, N.I., 1982. Seismic velocities. In Carmichael, R.S. (Ed.), *Handbook of Physical Properties of Rocks*: Boca Raton, FL (CRC Press), 2:1-228.
- Gillis, K.M., Mével, C., Allan, J.F., et al., 1993. *Proc. ODP, Init. Repts.*, 147: College Station, TX (Ocean Drilling Program).
- Karson, J.A., and Dick, H.J.B., 1983. Tectonics of ridge-transform intersections at the Kane Fracture Zone. *Mar. Geophys. Res.*, 6:51-98.
- Liou, J.G., Kuniyoshi, S., and Ito, K., 1974. Experimental studies of the phase relations between greenschist and amphibolite in a basaltic system. *Am. J. Sci.*, 274:613-632.
- Mével, C., Cannat, M., Gente, P., Marion, E., Auzende, J.-M., and Karson, J.A., 1991. Emplacement of deep crustal and mantle rocks on the west median valley wall of the MARK area (MAR 23°N). *Tectonophysics*, 190:31-53.
- Pezard, P.A., Howard, J.J., and Goldberg, D., 1991. Electrical conduction in oceanic gabbros, Hole 735B, Southwest Indian Ridge. In Von Herzen, R.P., Robinson, P.T., et al., *Proc. ODP, Sci. Results*, 118: College Station, TX (Ocean Drilling Program), 323-332.
- Robinson, P.T., Von Herzen, R., et al., 1989. *Proc. ODP, Init. Repts.*, 118: College Station, TX (Ocean Drilling Program).
- Shipboard Scientific Party, 1993. Explanatory notes. In Gillis, K., Mével, C., Allan, J., et al., *Proc. ODP, Init. Repts.*, 147: College Station, TX (Ocean Drilling Program), 15-42.
- Spear, F.S., 1981. An experimental study of hornblende stability and compositional variability in amphibolite. *Am. J. Sci.*, 281:697-734.

\*Abbreviations for names of organizations and publications in ODP reference lists follow the style given in *Chemical Abstracts Service Source Index* (published by American Chemical Society).

Ms 153IR-106

**NOTE:** For all sites drilled, core-description forms ("barrel sheets"), and core photographs can be found in Section 3, beginning on page 277. The CD-ROM (back pocket, this volume) contains the complete set of spreadsheets with piece-by-piece data for all structural features identified and measured. A set of summary spreadsheets that are linked to the igneous and metamorphic spreadsheets are also contained on the CD-ROM. Keys, summary tables, checklists, and thin-section summaries and notes are also archived. Compressed versions of the figures created for this volume, compatible with Macintosh computers, are located in the directories labeled REPT92X in the "Structure" directory. Scanned TIFF images of all the SVCD drawings are archived in the "STRCDRAW" file. Apparent dip data and true strike and dip data for all measurable features are contained in the "STR\_DIP" subdirectory. This directory also contains the LinesToPlane documentation and program that converts the apparent dip data to true strike and dip in an archived form. GRAPE, MST, and index properties are also reported on the CD-ROM.